Environmental Engineering and Management Journal

March 2015, Vol.14, No.3, 587-593
http://omicron.ch.tuiasi.ro/EEMJ/

"Gheorghe Asachi" Technical University of Iasi, Romania

GREEN SYNTHESIS AND CHARACTERIZATION OF GOLD NANOPARTICLES OBTAINED BY A DIRECT REDUCTION METHOD AND THEIR FRACTAL DIMENSION

Razvan State[1,2*], Florica Papa[2], Gianina Dobrescu[2], Cornel Munteanu[2], Irina Atkinson[2], Ioan Balint[2], Adrian Volceanov[1]

[1]University "Politehnica" of Bucharest, 313 Splaiul Independentei, Bucharest, Romania
[2]"Ilie Murgulescu" Institute of Physical Chemistry of the Romanian Academy, 202 Splaiul Independentei, Bucharest, Romania

Abstract

Nanoparticles are very interesting materials due to their properties which can be different than those of the bulk and they have many applications in various domains, like electronic, catalytic or biomedical. Gold is one of the most studied materials and is used in many applications that will have the human being as recipient, that's why gold nanoparticles should be obtained as environmentally friendly as possible. In this work, particles of around 50 nm were obtained in a so called "green" way by simply adding a solution containing the gold precursor ($HAuCl_4$) in a tannic acid solution. It was found that the amount of gold added in the tannic acid is directly proportional with the size of the obtained nanoparticles.

Key words: fractal dimension, gold nanoparticles, green synthesis

Received: November, 2014; Revised final: March, 2015; Accepted: March, 2015

1. Introduction

Due to their nanosized dimensions, nanoparticles have witnessed an increasing interest in the last decade becoming one of the most studied fields in the scientific community (Ahmad and Khan, 2013; Granmayeh Rad et al., 2011). Nanosized metal materials are the subject of many scientific researches due to their characteristic surface properties which are different from those of the bulk material. Great interest was focused on the noble metals nanoparticles (Kumari et al., 2013; Zhang et al., 1999). Gold is one of the most studied materials (Aswathy and Philip, 2012; Bratescu et al., 2013; Kyrychenko et al., 2011; Lee et al., 2007; Sárkány et al., 2008; Zabetakis et al., 2012) due to its unique optical, catalytic and spectroscopic properties.

The obtaining of Au nanoparticles becomes an important topic in different applications because the physical and chemical properties of the particles depend on their shape and size. Generally Au nanoparticles were synthesized by reducing $HAuCl_4$ with different reduction agents in the presence of some stabilizers (Hamaguchi et al, 2010; Kaur et al., 2012; Peng et al., 2008; Xu et al., 2013; Zhang and Toshima, 2012; Zhou et al., 2009; Zhu et al., 2005). Greener, environmentally friendly methods for the obtaining of metal nanoparticles are nowadays goal for a vast number of scientists in modern nanotechnology field.

Tannic acid is a polyphenolic compound derived from plants. It has antioxidant, antimutagenic and anticancer properties and it also reduces triglycerides. Besides its multipurpose applications it has been used also as a reducing agent and a protective colloid in noble nanoparticle synthesis (Ahmad et al., 2013; Ahmad, 2014; Yi et al., 2011). At its natural pH, tannic acid behaves as a weak

* Author to whom all correspondence should be addressed: e-mail: rstate@icf.ro, razvan.state@yahoo.com; Phone: 0721274801

reducing agent which can induce growth of nanoparticles at room temperature. Room temperature synthesis of silver or gold nanoparticles using tannic acid has been demonstrated recently by (Sivaraman et al., 2010) and long before (Ostwald et al., 1917) showed that tannin can reduce chloroauric acid at neutral pH to form stable gold nanoparticles even if tap water is used to prepare the aqueous solutions. Thus, tannic acid can be considered as an environmentally friendly reducing agent.

The goal of this work is to carry out: (a) synthesis of gold nanoparticles with various amounts of $HAuCl_4$, by a direct and environmentally friendly reduction method of the gold precursor solution with tannic acid; (b) analysis of the influences of how the gold precursor was added, on the size and shape of the obtained gold nanoparticles; (c) structural and morphologic characterization by different techniques of the synthesized gold nanoparticles.

2. Materials and methods

Chloroauric acid ($HAuCl_4 \cdot 4H_2O$) was provided by Wako Pure Chemical Industry, Ltd. and tannic acid ($C_{34}H_{28}O_{21}$) from Carl Roth GmbH. All the solutions for the synthesis of gold nanoparticles in this paper were freshly prepared using demineralised water.

The as obtained nanoparticles were characterized through XRD spectroscopy. The XRD patterns were collected by means of a Rigaku diffractometer type Ultima IV in parallel-beam geometry. The source of the X-rays was a Cu tube (λ = 0.15418 nm) operating at 40 kV and 30 mA. Counts were collected from 10º to 80º with a step size of 0.02 and a speed of 5º/min. Rigaku's PDXL software package, connected to the ICDD database was used for the phase identification. Transmission electron microscopy (TEM) was performed on FEI Tecnai G2-F30 S-Twin field-emission gun scanning transmission electron microscope (FEG STEM) operating at 300 kV. A drop of the nanoparticles suspension was mounted on a holey carbon film copper grid allowing the solvent to evaporate at room temperature. UV-VIS spectra were performed using an Analytic Jena Specord 200 plus apparatus.

3. Experimental

Until now, the majority of the obtained materials using similar synthesis aimed particle size up to 20 nm. In this work, gold nanoparticles of around 50 nm were obtained very simple, through a direct and environmentally friendly reduction method. The gold precursor consisted in a water based solution of chloroauric acid of 0.9 mM. After obtaining of the gold precursor, it was injected in a water based solution of tannic acid of 0.9 mM according to scheme presented in Fig. 1. Firstly, two sample batches were prepared. In one of them 15 mL of the as obtained gold precursor solution was injected slowly, using a dropping funnel, in 15 mL of tannic acid solution, sample Au1 (molar ratio Au: tanic acid 1:1) and in the second one, 35 mL of gold precursor solution was injected also slowly into 15 mL solution of tannic acid, sample Au2 (molar ratio Au: tanic acid 2.3:1).

The tannic acid solution was kept in both cases under magnetic stirring. The reduction occurs almost instantly. In the case of 1:1 ratio (Au1) the solution turns dark blue and in the second case, 2.3:1 (Au2) the solution turns in a brown-red (muddy red) color. Both solutions were kept under stirring for a better homogenization and then the synthesized nanoparticles were recovered. The recovery was made by using a 4000 RPM centrifuge device. After separation, the obtained powder was calcinated at 200 °C for 2 hours. A third sample of 2.3:1 ratio was prepared following the same protocol with the exception that the gold precursor solution was injected rapidly in the tannic acid solution, sample Au3. The obtained solution was also muddy red. After recovery, all the samples were characterized through TEM and XRD analyses. UV-Vis spectra were obtained for the prepared solutions prior to nanoparticle recovery.

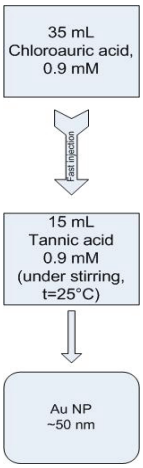

Fig. 1. Schematic representation of gold nanoparticles synthesis, sample A3

4. Results and discussion

The reduced gold solutions were analyzed by UV-Vis spectroscopy (Fig. 2), prior to nanoparticle recovery. It can easily be seen that the as obtained gold nanoparticles have a good adsorption in the visible range, with the 2.3:1 sample having a bigger adsorption that the 1:1 sample.

In order to observe the morphology, size and shape of the synthesized Au nanoparticles all 3 samples were subjected to TEM analysis. It was observed that the Au nanoparticles are faceted (Fig. 3), with a size ranging from 20 to 50 nm, depending on the amount of gold precursor added in the tannic acid solution. Unfortunately the dispersion in the first 2 samples was rather poor (Fig. 4), but this was solved in the third sample when the injection mechanism was changed.

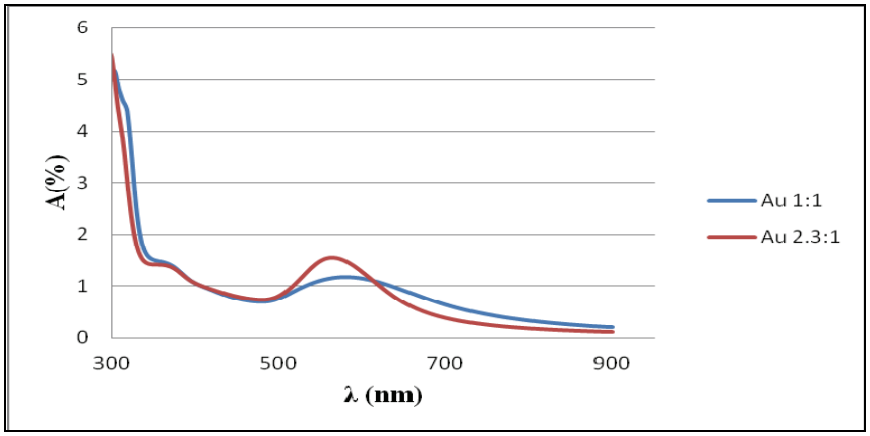

Fig. 2. UV-Vis spectra of the reduced gold solutions

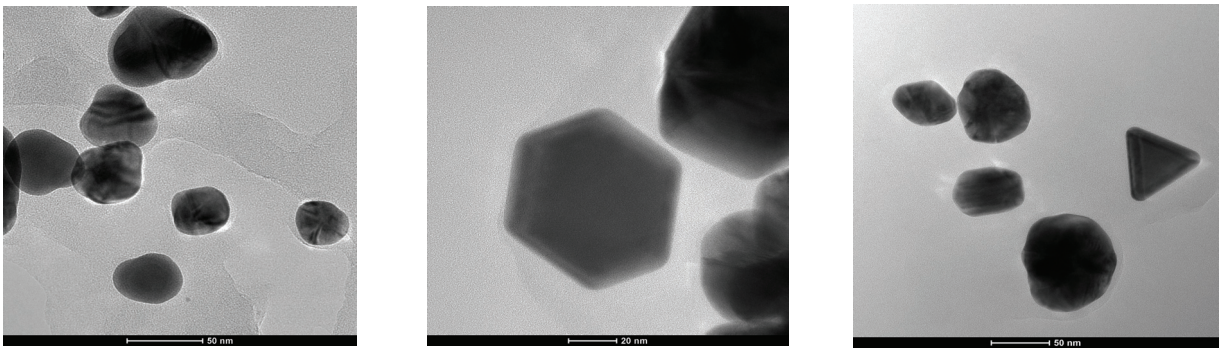

a) **b)** **c)**

Fig. 3. TEM images of: a) Au1, b) Au2 sample and c) Au3

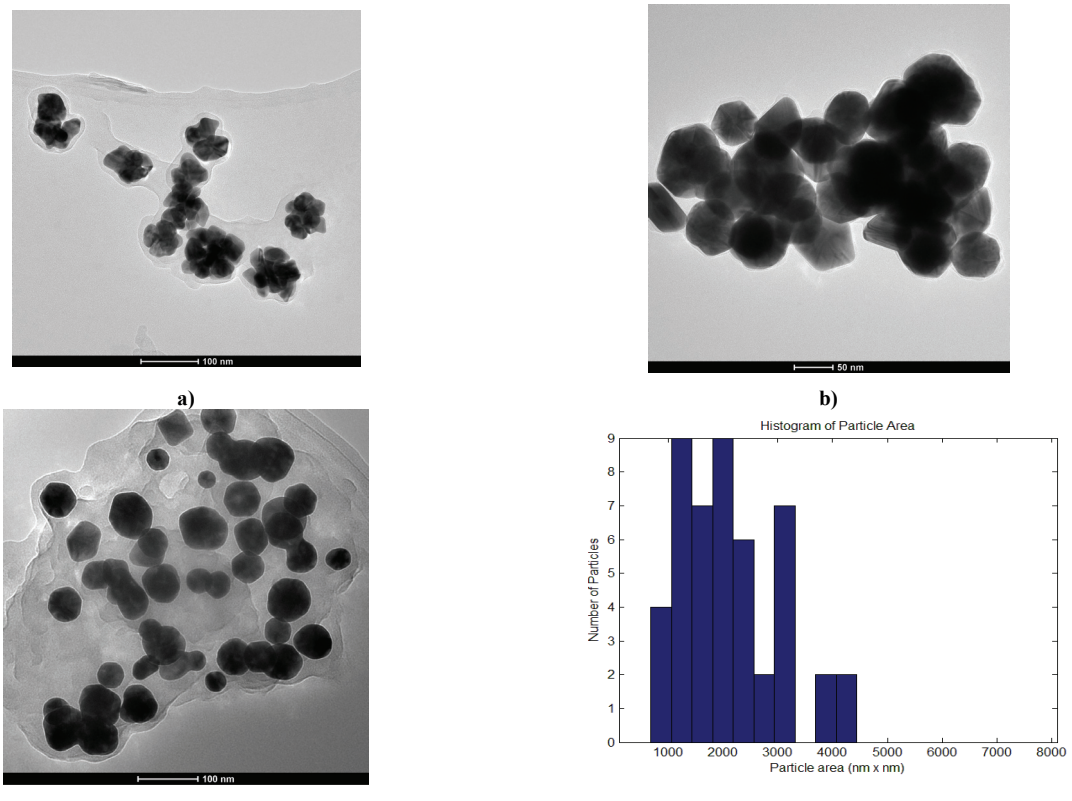

a) **b)** **c)** **d)**

Fig. 4. TEM images showing the nanoparticle dispersion of a) Au1 sample, b) Au2 sample and c) Au3 sample. Histogram of particle area (d) of Au3 sample

In Fig 4 one can see that the dispersion is much better for the sample Au3 then in the case of the other 2 where the chloroauric solution was slowly added in the tannic acid. When analyzing the particle area one can see that the majority of the particles have a surface area between 1500 and 3000 nm^2, making them suitable for many applications, including catalysis. Unfortunately the shape is inconclusive. They are faceted, some of them are triangles or hexagons (Fig. 3) but the majority has an undefined shape.

TEM images were also analyzed using the fractal theory (Mandelbrot, 1977). A *fractal* is an object whose observed volume depends on the resolution (length scale) at several orders of magnitude and follows a power law behavior with a nontrivial exponent; it has the property of self-similarity. The fractal dimension was computed using three methods: the correlation function method, the variable length scale method and the box-counting method. The first two methods were carried out using personal computer codes, meanwhile the last one using Benoit Soft, version 1.31, TruSoft Int'l, Inc.

Self-similarity has a mathematical description given by Eq. (1), where: D is the fractal dimension and $N(r, R)$ is the number of boxes of size r which cover the object of linear size R; in other words, self-similarity is the property of an object to look the same when zooming in (Mandelbrot, 1977; Mandelbrot, 1982).

$$N(r/R) \sim (r/R)^{-D} \quad (1)$$

Keeping constant the maximum size of the object R, the box dimension is defined as the exponent D in Eq. (2), where: $N(r)$ is the number of boxes of linear size r necessary to cover the object in a two-dimensional plane.

$$N(r) = Ar^{-D} \quad (2)$$

For Euclidean objects, one needs a number of boxes proportional to r^{-D}, so the exponent D is the Euclidean dimension of the plane, 2. The prefactor A, sometimes named lacunarity, is a measure of how the space is filled, a measure of the gap or of the object texture (Lapuerta et al., 2010). The grey level of each image pixel was converted in height and the fractal dimension of the equivalent surface was computed using two methods: the height correlation function method and the variable length scale method.

The first method (Family and Vicsek, 1985) uses the height correlation function according to Eq. (3), where: the symbol <…> denotes an average over x.

$$G(r) \equiv < \left[h(\vec{x}) - h(\vec{x}+\vec{r})\right]^2 >_x \quad (3)$$

Thus the height correlation function $G(r)$ obeys the following scaling relation for a surface embedded in a 3-dimensional Euclidean space (Eq. 4).

$$G(r) \sim r^{2(3-D)}, r << L \quad (4)$$

The scaling range where equation (4) is valid defines the "cut-off" limits and indicates the range of self-affinity, in other words, the range where there are correlations between surface points. The second method was proposed by (Chauvy et al., 1998) and consists in computing the rms deviation of the surface. The algorithm is the following: (i) an interval of length ε in case of a profile, (or a box of size ε x ε in case of a surface) is defined; (ii) a linear (or planar) least square fit on the data within the interval is performed and the roughness is calculated; (iii) the interval (box) is moved along the profile (surface) and step (ii) is repeated; (iv) the rms deviation for multiple intervals is computed, and (v) steps (ii)-(iv) are repeated for increasing lengths (box sizes).

Rms deviation $R_{q\varepsilon}$, averaged over n_ε, the number of intervals of length ε, is defined by Eq. (5), where: z_j is the jth height variation from the best fit line within the interval i, and p_ε is the number of points in the interval ε.

$$R_{q\varepsilon} = \frac{1}{n_\varepsilon}\sum_{i=1}^{n_\varepsilon}\sqrt{\frac{1}{p_\varepsilon}\sum_{j=1}^{p_\varepsilon} z_j^2} \quad (5)$$

The log-log plot of $R_{q\varepsilon}$ versus ε gives the Hurst or roughening exponent H, and the fractal dimension D, can be calculated as given by Eq. (6), where: D_T is the topological dimension of the embedding Euclidean space (D_T=2 for profiles and D_T=3 for surfaces).

$$D = D_T - H \quad (6)$$

The variable length scale method is more suitable for higher scaling range than the correlation function method because of the necessity to have enough points in an interval ε x ε to compute rms deviation $R_{q\varepsilon}$, averaged over n_ε, meaning that ε must be high enough for a good statistic.

The last two methods describe the fractal properties of the equivalent surfaces defined by the gray-level of each pixel converted into height, meanwhile the box-counting method describes the fractal properties of an equivalent image obtained from conversion of the gray scaled image into a black and white one. The results are presented in Tables 1-3.

The samples have fractal behavior as all methods shows. The Au1 sample is characterized, as an equivalent surface, by three fractal dimensions: 2.40, 2.63 and 2.34, indicating that the nanoparticles are agglomerated in correlated clusters. The Au2 sample is also characterized by three fractal dimensions: 2.31, 2.55 and 2.15. The first two fractal dimensions indicate correlations between points on each nanoparticle, meanwhile the last one shows the

existence of a single cluster, with a global fractal behavior characterized by a low fractal dimension and strong agglomeration. The Au3 sample is characterized by two fractal dimensions: 2.48-2.58 for correlations between points on each nanoparticle and 2.30, characterizing correlations between nanoparticles themselves. The dispersion in the fractal values 2.48-2.58 is a result of some overlapping nanoparticles and of the projection of a 3-dimensional structure onto the 2-dimensional image.

The box-counting fractal dimension of the black-and-white image for the Au1 sample has two values: 1.83 at short scale and 1.35 at a large scale. The first values indicates correlations between nanoparticles in a cluster, meanwhile the second one indicates the correlation between clusters. It is very interesting to notice that the first value of 1.83 is very closed to Sutherland's simulations D=1.85 (Stanley, 1977; Sutherland, 1967; Sutherland, 1970; Sutherland and Goodarz-Nia, 1971).

The model was developed for colloidal aggregation and suppose that the single particles aggregate one with each other and then to form binary clusters, the binary clusters aggregate one with each other, and so on. In our case, the slowly gold precursor solution injection will favor aggregation, as diffusion is not a leading mechanism in the system. The box-counting fractal dimension of the Au2 sample is 1.87, again, very close to the Sutherland's value of 1.85. The box-counting fractal dimension of the Au3 sample is 1.79 very closed to the 1.78 value obtained from diffusion limited cluster-cluster aggregation simulations (Meakin, 1986) in the aggregation of gold colloids (Weitz and Oliveira, 1984), when rapid aggregation is involved and diffusion is a leading mechanism, the fractal dimension will lead to the 1.75 value, very close to our 1.79.

Table 1. Nanoparticle fractal dimensions of Au1 sample

Method	***Fractal dimension***	***Determination Coefficient***	***Self-similarity domain (nm)***
Correlation method	2.40±0.01	0.999	2.5-29
Variable Length Scale Method	2.63±0.01 2.34±0.02	0.992 0.982	6-20 20-55
Box-Counting Method	1.83±0.01 1.35±0.04	0.999 0.995	0.4-24 24-115

In order to make sure of their composition, the synthesized gold nanoparticles were subjected to X-Ray diffraction analysis. The XRD diphractograms confirms the existance of metallic gold without the presence of any other impurities for all the studied samples. Fig. 5 shows the XRD patterns of Au1-Au3 samples. The XRD patterns reveal the presence of diffraction lines centred at 38.18º, 44.43º, 64.61º and 77.64º corresponding to (111), (200), (220) and (311) planes respectively of Au compound with cubic structure (JCPDS card no. 00-004-0784). The broad halo at around 2θ=20º in the diffraction patterns is the contribution of glass sample holder.

Table 2. Nanoparticle fractal dimensions of Au2 sample

Method	***Fractal dimension***	***Determination Coefficient***	***Self-similarity domain (nm)***
Correlation method	2.31±0.01	0.999	2.6-13
Variable Length Scale Method	2.55±0.03 2.15±0.03	0.981 0.994	4-13 13-56
Box-Counting Method	1.87±0.01	0.999	0.3-119

Table 3. Nanoparticle fractal dimensions of Au3 sample

Method	***Fractal dimension***	***Determination Coefficient***	***Self-similarity domain (nm)***
Correlation method	2.48±0.01	0.995	2-20
Variable Length Scale Method	2.58±0.01 2.30±0.01	0.996 0.990	6-17 17-89
Box-Counting Method	1.79±0.01	0.999	1-151

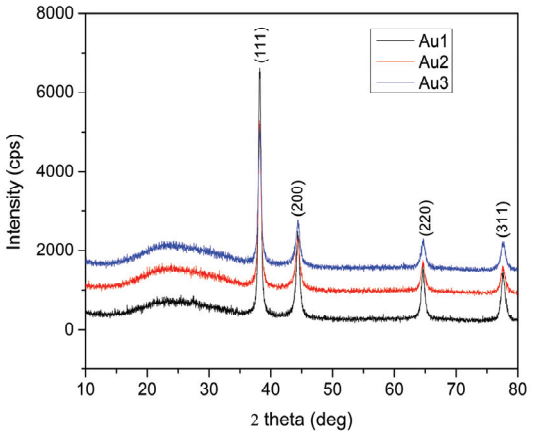

Fig. 5. XRD spectra of the synthesized gold nanoparticles

5. Conclusions

Gold nanoparticles of 20 to 50 nm were obtained using a simple and in the same time an environmentally friendly synthesis method. In the first two samples only the amount of added gold precursor is different, the synthesis mechanism being identical. It was observed that the dimension of the

obtained nanoparticles is directly proportional with the amount of gold added in the tannic acid. Because the dispersion of the synthesized nanoparticles is rather poor, a third sample was made, keeping the quantities used in the second sample but changing the injection mechanism. Thus, rapidly injecting the precursor solution in the reducing one, we obtained a better dispersion of the nanoparticles than it was obtained by slowly adding the chloroauric acid aqueous solution in the tannic acid solution. We used the proportions of the second sample because we needed to obtain nanoparticles with average size around 50 nm. Even though the shape of the as obtained particles is not homogenous, we saw from the UV-Vis spectra that all the samples adsorb in the visible range.

Fractal analysis of TEM images indicate the same behavior: the first two samples are correlated clusters of nanoparticles, with low dispersion and highly agglomerated, characterized by three fractal dimensions, meanwhile the last one consist of a self-similar structure of nanoparticles with high dispersion, and two characteristic fractal dimensions. The box-counting fractal dimension values offer some information about the synthesis mechanism: slow injection can be simulated by the colloidal aggregation; meanwhile the rapid injection is well described by the diffusion limited cluster-cluster aggregation model. Also, from the XRD spectra it was clear that all the obtained materials consist only in metallic gold.

Therefore, these nanoparticles, obtained by a so called 'green synthesis' are suitable for further analysis and testing in many applications, including catalytic and photo catalytic tests for a current worldwide problem consisting in the removal of nitrite from water (Bulgariu et al., 2012), which is the goal of our future study.

Acknowledgements

This work was supported by Project SOP HRD - PERFORM /159/1.5/S/138963, PN2 100/2012 INTEGRATREAT and PN2 46/2012 BICLEANBIOS.

References

Ahmad T., (2014), Reviewing the tannic acid mediated synthesis of metal nanoparticles, *Journal of Nanotechnology,* ID 954206, http://dx.doi.org/10.1155/2014/954206.

Ahmad T., Khan W., (2013), Size variation of gold nanoparticles synthesized using tannic acid in response to higher chloroauric acid concentrations, *World Journal of Nano Science and Engineering*, **03**, 62-68.

Aswathy A.S., Philip D., (2012), Facile one-pot synthesis of gold nanoparticles using tannic acid and its application in catalysis, *Physica E: Low-dimensional Systems and Nanostructures*, **44**, 1692-1696.

Bratescu MA., Takai O., Saito N., (2013), One-step synthesis of gold bimetallic nanoparticles with various metal-compositions, *Journal of Alloys and Compounds*, **562**, 74-83.

Bulgariu L., Ceica A., Lazar L., Cretescu I., Balasanian I., (2012), Equilibrium and kinetics study of nitrate removal from water by Purolite A520-E resin, *Environmental and Management Journal*, **11**, 37-45.

Chauvy P.F., Madore C., Landolt D., (1998), Variable length scale analysis of surface topography: characterization of titanium surfaces for biomedical applications, *Surface and Coatings Technology*, **110**, 48-56.

Family F., Vicsek T., (1985), Scaling of the active zone in the Eden process on percolation networks and the ballistic deposition model, *Journal of Physics*, *A*, **18**, **1**, 75-82.

Granmayeh Rad A., Abbasi H., Hossein Afzali M., (2011), Gold nanoparticles: Synthesising, characterizing and reviewing novel application in recent years, *Physics Procedia*, **22**, 203-208.

Hamaguchi K., Kawasaki H., Arakawa R., (2010), Photochemical synthesis of glycine-stabilized gold nanoparticles and its heavy-metal-induced aggregation behavior, *Colloids and Surfaces A: Physicochemical and Engineering Aspects*, **367**, 167-173.

Kaur R., Pal B., (2012), Size and shape dependent attachments of Au nanostructures to TiO_2 for optimum reactivity of Au–TiO_2 photocatalysis, *Journal of Molecular Catalysis A: Chemical*, **355**, 39-43.

Kyrychenko A., Karpushina G.V., Bogatyrenko S.I., Kryshtal A.P., Doroshenko A.O., (2011), Preparation, structure, and a coarse-grained molecular dynamics model for dodecanethiol-stabilized gold nanoparticles, *Computational and Theoretical Chemistry*, **977**, 34-39.

Lapuerta M., Martos F.J., Martin-Gonzalez G., (2010), Geometrical determination of the lacunarity of agglomerates with integer fractal dimension, *Journal of Colloid and Interface Science*, **346**, 23–31.

Lee K.Y., Hwang J., Lee W., Kim J., Han S.W., (2007), One-step synthesis of gold nanoparticles using azacryptand and their applications in SERS and catalysis, *Journal of Colloid and Interface Science*, **316**, 476-481.

Mandelbrot B.B., (1977), *Fractals: Form*, *Chance and Dimension*, Freeman, San Francisco.

Mandelbrot B.B., (1982), *The Fractal Geometry of Nature*, Freeman, San Francisco, 14-19.

Meakin P., (1986), *Computer Simulation of Growth and Aggregation Processes*, In: *On Growth and Form*, Stanley H.E., Ostrowsky N. (Eds.), Martinus Nijhoff Publishers, 111-135.

Meena Kumari M., Aromal S.A., Philip D., (2013), Synthesis of monodispersed palladium nanoparticles using tannic acid and its optical non-linearity, *Spectrochimica Acta Part A: Molecular and Biomolecular Spectroscopy*, **103**, 130-133.

Ostwald W., (1917), *An Introduction to Theoretical and Applied Colloid Chemistry*, John Wiley and Sons New York.

Peng S., Lee Y., Wang C., Yin H., Dai S., Sun S.H.A., (2008), A facile synthesis of monodisperse Au nanoparticles and their catalysis of CO oxidation, *Nano Research*, **1**, 229-234.

Sárkány A., Geszti O., Safran G., (2008), Preparation of Pd shell–Au core/SiO_2 catalyst and catalytic activity for acetylene hydrogenation, *Applied Catalysis A: General*, **350**, 157-163.

Sivaraman S., Kumar S, Santhanam V., (2010), Room-temperature synthesis of gold nanoparticles – Size-control by slow addition, *Gold Bulletin*, **43**, 275-286.

Stanley H.E., (1977), Cluster shapes at the percolation threshold: and effective cluster dimensionality and its

connection with critical-point exponents, *Journal of Physics*, **10**, L211-L220.

Sutherland D.N., (1967), A theoretical model of floc structure, *Journal of Colloid and Interface Science*, **25**, 373-380.

Sutherland D.N., (1970), Chain formation of fine particle aggregates, *Nature*, **226**, 1241-1242.

Sutherland D.N., Goodarz-Nia I., (1971), Floc simulation: The effect of collision sequence, *Chemical Engineering Science*, **26**, 2071-2085.

Weitz D.A., Olivera M., (1984), Fractal structures formed by kinetic aggregation of aqueous gold colloids, *Physical Review Letters*, **52**, 1433-1436.

Xu F., Zhang Q., Gao Z., (2013), Simple one-step synthesis of gold nanoparticles with controlled size using cationic Gemini surfactants as ligands: Effect of the variations in concentrations and tail lengths, *Colloids and Surfaces A: Physicochemical and Engineering Aspects*, **417**, 201-210.

Yi Z., Li X., Xu X., Luo B., Luo J., Wu W., Yi Y., Tang Y., (2011), Green, effective chemical route for the synthesis of silver nanoplates in tannic acid aqueous solution, *Colloids and Surfaces A: Physicochemical and Engineering Aspects*, **392**, 131-136.

Zabetakis K., Ghann W.E., Kumar S., Daniel M.-C., (2012), Effect of high gold salt concentrations on the size and polydispersity of gold nanoparticles prepared by an extended Turkevich–Frens method, *Gold Bulletin*, **45**, 203-211.

Zhang H., Toshima N., (2012), Fabrication of catalytically active AgAu bimetallic nanoparticles by physical mixture of small Au clusters with Ag ions, *Applied Catalysis A: General*, **447-448**, 81-88.

Zhou J., Ralston J., Sedev R., Beattie D.A., (2009), Functionalized gold nanoparticles: synthesis, structure and colloid stability, *Journal of Colloid and Interface Science*, **331**, 251-262.

Zhu H., Pan Z., Hagaman E.W., Liang C., Overbury S.H., Dai S., (2005), Facile one-pot synthesis of gold nanoparticles stabilized with bifunctional amino/siloxy ligands, *Journal of Colloid and Interface Science*, **287**, 360-365.